RARE METALS
Vol. 29, No. 2, Apr 2010, p. 149
DOI: 10.1007/s12598-010-0026-2

Preparation of new sunscreen materials $Ce_{1-x}Zn_xO_{2-x}$ via solid-state reaction at room temperature and study on their properties

WU Wenwei, LI Shushu, LIAO Sen, XIANG Feng, and WU Xuehang

School of Chemistry and Chemical Engineering, Guangxi University, Nanning 530004, China

Received 6 March 2009; received in revised form 7 May 2009; accepted 15 May 2009

Abstract

Superfine cerium-zinc oxides $Ce_{1-x}Zn_xO_{2-x}$ with x = 0, 0.1, 0.3, 0.5, and 1.0 were obtained by grinding $Ce(SO_4)_2{\cdot}4H_2O$, $ZnSO_4{\cdot}7H_2O$ and NH_4HCO_3 under the condition of surfactant PEG-400 being present at room temperature, washing the mixture with water to remove soluble inorganic salts, drying at 80°C, and calcining. The precursor and its calcined samples were characterized using thermogravimetry and differential thermal analyses (TG/DTA), UV-vis absorption spectroscopy, X-ray powder diffraction (XRD), and scanning electron microscopy (SEM). The results showed that superfine $Ce_{1-x}Zn_xO_{2-x}$ behaved as an excellent UV-shielding material. The ZnO-doped CeO_2 can facilitate the formation of crystalline state CeO_2. The catalytic ability of products used in air oxidation of castor oil was investigated. The results showed that the catalytic abilities of products decreased with increasing zinc amount.

Keywords: cerium oxide; zinc oxide; solid-state reaction; UV absorbency; catalytic properties

1. Introduction

It has been well known that ultraviolet (UV) rays in sunlight cause several problems such as photodegradation of organic materials and damaging human health (causing sunburn, acceleration of aging, causing cancer, and so on) [1-3]. Therefore, excellent sunscreen materials for UV-shielding have received considerable attention, and some progress has been made [2-13]. Ultrafine ceria (CeO_2) has ideal characteristics for use as a broad-spectrum inorganic sunscreen in personal-care products: it is relatively transparent to visible light, but has excellent ultraviolet radiation absorption properties [6]. However, because of its high catalytic activity for the oxidation of organic materials, ceria has seldom been used commercially as a sunscreen material. Therefore, how to prepare low catalytic activity ceria powder with excellent ultraviolet radiation absorption properties is a key for application. It was found that the catalytic activity of ceria can be related with the oxygen release, and the oxygen release may be depressed by doping with metal ion possessing both larger ionic size and lower valence than Ce^{4+} to stabilize the fluorite structure of ceria [14]. Therein, Ca^{2+} and Zn^{2+} ions were widely used as doped ions. The catalytic ability of calcia-doped ceria was decreased substantially by coating with silica shell, but its UV-shielding ability also decreased substantially, which is attributed to the presence of a number of calcia and silica of no UV-shielding ability [13, 15]. Li *et al.* [14] found that zinc oxide-doped ceria showed as excellent UV absorption and transparency in the visible ray region in a similar manner as that of the undoped ceria, but zinc oxide-doped ceria substantially decreased the catalytic activity. The two kinds of doped ceria described above were synthesized via soft solution chemical routes at 40°C when $CeCl_3$, $CaCl_2$, and $ZnCl_2$ were used as raw materials, and NaOH and hydrogen peroxide were used as a precipitator and oxidant, respectively. The process was rigorous and it was not easy to prepare the product on a large scale.

Solid-state reaction at room temperature or near room temperature (< 40°C) is a novel synthetic technique that has been developed in the past twenty years [16]. It has received considerable attention because of its simplicity, low cost, high output and little pollution in addition to easily preparing superfine materials by this method. This paper reports on the preparation of superfine $Ce_{1-x}Zn_xO_{2-x}$ with x = 0, 0.1, 0.3, 0.5, and 1.0 via solid-state reaction at room temperature when $Ce(SO_4)_2{\cdot}4H_2O$, $ZnSO_4{\cdot}7H_2O$, and NH_4HCO_3 were used as raw materials. The results showed that the precursor decomposed into superfine Zn^{2+}-doped CeO_2 with excellent UV-shielding ability below 150°C, and the catalytic ability

Corresponding author: WU Wenwei **E-mail:** gxuwuwenwei@126.com

of products for air oxidation of castor oil was decreased substantially.

2. Experimental

2.1. Reagent and apparatus

All chemicals were of reagent-grade purity. TG/DTA measurements were made using a Netsch 40 PC thermogravimetric analyzer. X-ray powder diffraction (XRD) was performed using a Rigaku D/max 2500 V diffractometer equipped with a graphite monochromator and a Cu target. The UV-vis diffuse reflectance spectra of the prepared and calcined samples were recorded on a UV-2501 IPC instrument using integrated sphere and $BaSO_4$ powder was employed as a reference. The morphology of the product was examined by S-3400 scanning electron microscopy (SEM).

2.2. Preparation of $Ce_{1-x}Zn_xO_{2-x}$

The dosage of Ce and Zn was fixed to 20 mmol, and that of surfactant PEG (polyethylene glycol)-400 was 600 μL in the experiment. The synthetic procedure was as follows: The $Ce(SO_4)_2{\cdot}4H_2O$, $ZnSO_4{\cdot}7H_2O$, NH_4HCO_3, and surfactant PEG-400 were placed in a mortar. The mixture was fully ground by hand with a rubbing mallet for 40 min. The grinding velocity was about 90 r/min and the strength was moderate. The reactant mixture gradually became damp, and then a paste formed quickly. The mixture was washed with water to remove soluble inorganic salts until SO_4^{2-} ion could not be visually detected with a 0.5 $mol{\cdot}L^{-1}$ $BaCl_2$ solution. The solid was then washed with a small quantity of anhydrous ethanol and dried at 80°C for 3 h to give the precursor of $Ce_{1-x}Zn_xO_{2-x}$. The $Ce_{1-x}Zn_xO_{2-x}$ powder was obtained via thermal decomposition of the precursor.

2.3. Catalytic ability of products

The catalytic ability for oxidation of organic material was determined by conductometric determination method (Rancimat method) [17] using castor oil of reagent-grade as oxidizing material. The sample powder (1.0 g) was mixed with castor oil (10.0 mL) and followed by blast air with 566 mL/min at 125°C, where the air was introduced into deionized water. The catalytic ability was determined by measuring the increase in the electric conductivity of deionized water by trapping the volatile molecules coming from the oxidation of castor oil on heating.

3. Results and discussion

3.1. TG/DTA analysis of $Ce_{1-x}Zn_xO_{2-x}$ precursor

Fig. 1 shows the TG/DTA pattern of $Ce_{1-x}Zn_xO_{2-x}$ precursor (with x = 0 and 1) when heated at a rate of 10°C/min from ambient temperature to 725°C. From Fig. 1(a), the DTA curve shows that thermal decomposition of CeO_2 precursor below 725°C occurs at an endothermic peak and an exothermic peak. The broad endothermic DTA peak at 96.8°C is attributed to the dehydration of adsorption water or hydroxide. The exothermic peak, which is located at 486.6°C, is related to the elimination of oxygen gas from decomposition of CeO_2 and formation of Ce_2O_3 [12]. From Fig. 1(b), the DTA curve shows that thermal decomposition of ZnO precursor below 725°C occurs at an endothermic peak. The endothermic peak at 264.1°C is attributed to thermal decomposition of $ZnCO_3$ and the formation of crystalline ZnO [18].

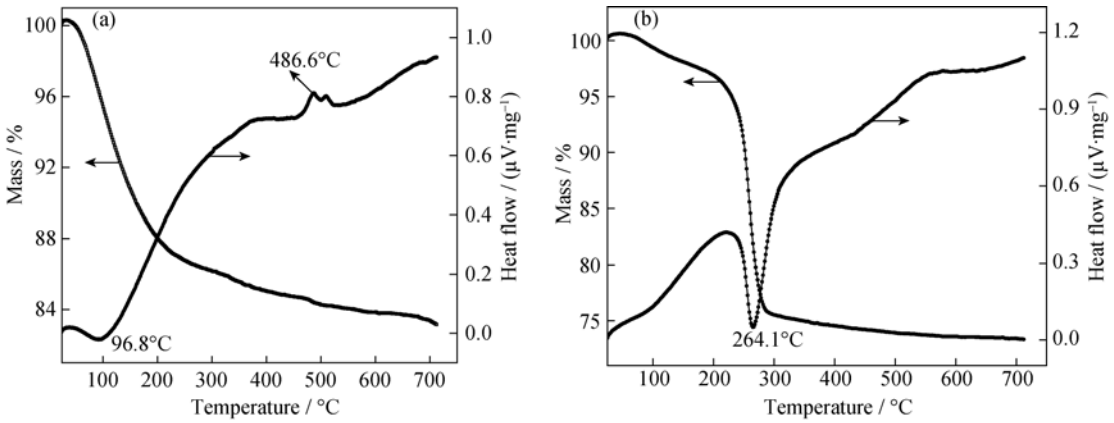

Fig. 1. TG/DTA patterns of $Ce_{1-x}Zn_xO_{2-x}$ precursor: (a) x = 0; (b) x = 1.

3.2. UV-vis analysis of the precursor and calcined samples

The UV-vis absorption spectra of the precursor and calcined samples are presented in Fig. 2. It can be seen that all the samples obtained at 80°C have strong UV absorbing between 280 and 400 nm and their absorbency exceeds 1.60 except ZnO. The absorbency of $Ce_{1-x}Zn_xO_{2-x}$ between 280

and 400 nm changes with x and calcination temperature. Therein, the UV absorbency of samples obtained from calcining $ZnCO_3$ is markedly influenced by calcining temperature, which is because the sample obtained below 300°C is $ZnCO_3$, and the sample obtained above 300°C is ZnO [18]. In order to compare the UV absorbing ability between samples with different compositions quantitatively, the dependence of UV absorbency peak area between 280 and 400 nm for $Ce_{1-x}Zn_xO_{2-x}$ on calcination temperature is given in Fig. 3. The results show that UV absorbency peak area between 280 and 400 nm for $Ce_{1-x}Zn_xO_{2-x}$ decreases with an increase of calcination temperature on the whole, which is because particle size of CeO_2 powder increases with the increase of calcining temperature, and amorphous particles can be easily transformed into crystalline states. These facts were confirmed by XRD analysis. However, authors think the change of the crystallinity is dominant. The larger the UV absorption peak area, the stronger the UV absorbency, and thus, $Ce_{0.9}Zn_{0.1}O_{1.9}$ obtained at 150°C has the strongest ultraviolet absorption ability.

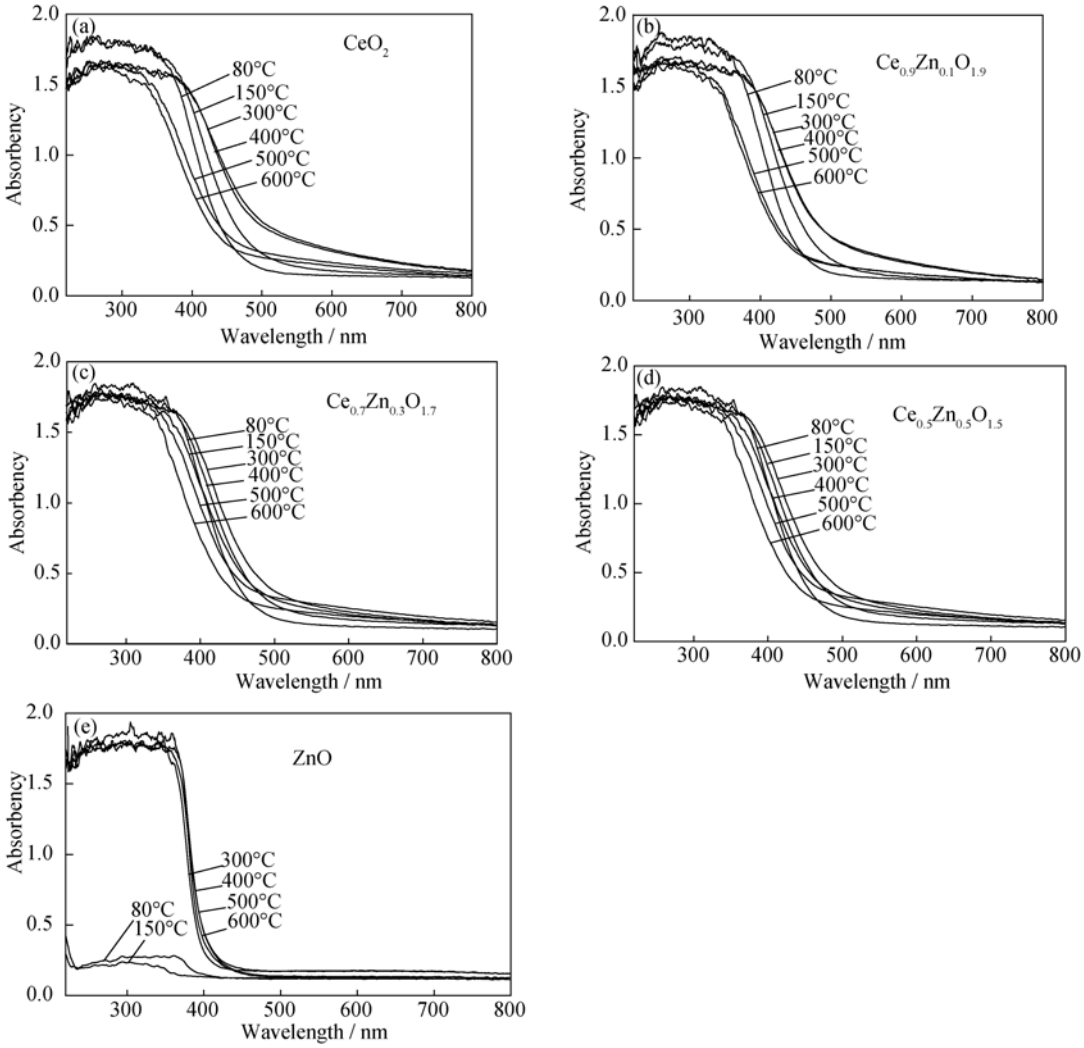

Fig. 2. UV-vis absorption spectra of $Ce_{1-x}Zn_xO_{2-x}$ samples calcined at different temperatures for 2 h: (a) CeO_2; (b) $Ce_{0.9}Zn_{0.1}O_{1.9}$; (c) $Ce_{0.7}Zn_{0.3}O_{1.7}$; (d) $Ce_{0.5}Zn_{0.5}O_{1.5}$; (e) ZnO.

3.3. XRD analysis of the calcined samples

Fig. 4 shows the XRD patterns of the calcined samples at different temperatures for 2 h. Fig. 4(a) shows that the structure of CeO_2 particles obtained below 300°C is amorphous. However, the characteristic diffraction peaks of crystalline CeO_2 appear when it is kept at 400°C for 2 h, and its degree of crystallinity increases with calcination temperature, for example, the resulting particle sizes of CeO_2 from calcining CeO_2 at 400, 500, and 600°C are 12, 13, and 17 nm, respectively. In Fig. 4(b) and Fig. 4(c), the characteristic diffraction peaks of crystalline CeO_2 appear when $Ce_{0.7}Zn_{0.3}O_{1.7}$ and $Ce_{0.5}Zn_{0.5}O_{1.5}$ samples are heated at 300 and 150°C, respectively. It is explained by the fact that

ZnO-doped CeO_2 can facilitate formation of crystalline state CeO_2. The exact crystallization mechanisms of CeO_2 in the presence of ZnO are not clear. No characteristic diffraction peaks of crystalline ZnO appear at all the calcination temperatures, and it is confirmed that ZnO forms a solid solution with CeO_2.

3.4. SEM analysis of $Ce_{1-x}Zn_xO_{2-x}$ samples

The SEM micrographs of $Ce_{1-x}Zn_xO_{2-x}$ obtained at 300°C for 2 h are shown in Fig. 5. It can be seen that all products have near spherical shapes, and there is a soft agglomeration phenomenon in the particles of samples. The average particle diameters of CeO_2, $Ce_{0.7}Zn_{0.3}O_{1.7}$, and $Ce_{0.5}Zn_{0.5}O_{1.5}$ are about 75, 90, and 100 nm, respectively.

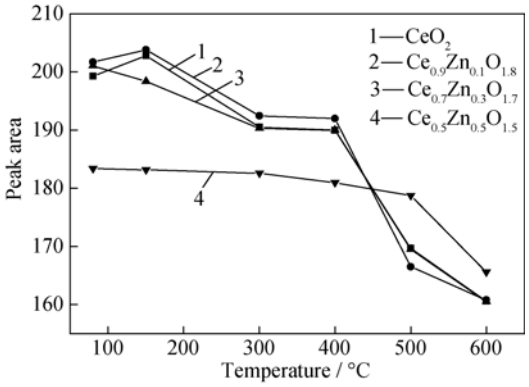

Fig. 3. Dependence of the UV absorption peak area of $Ce_{1-x}Zn_xO_{2-x}$ on calcination temperature.

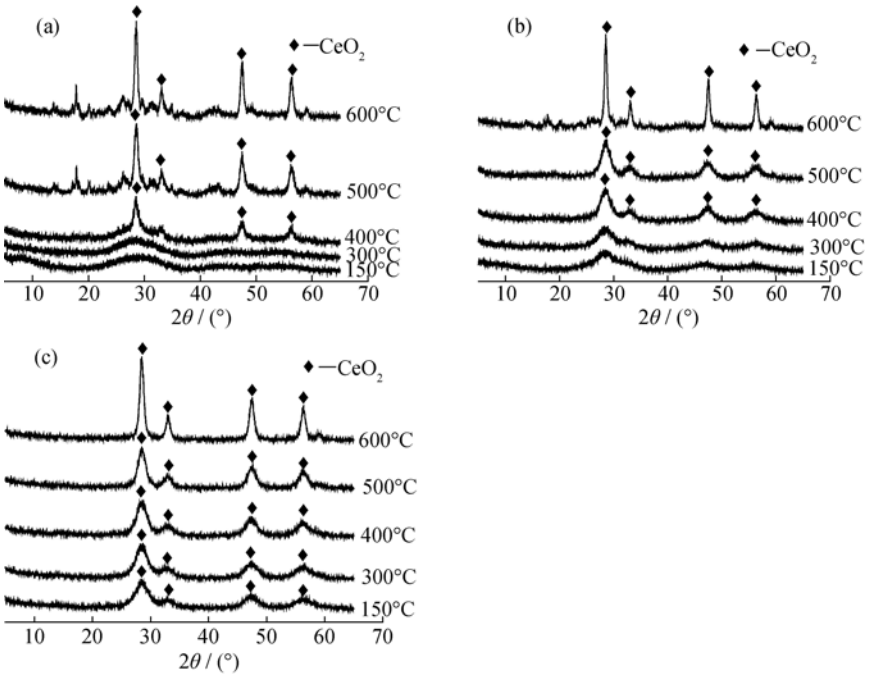

Fig. 4. XRD patterns of $Ce_{1-x}Zn_xO_{2-x}$ obtained at different temperatures for 2 h: (a) $x = 0$; (b) $x = 0.3$; (c) $x = 0.5$.

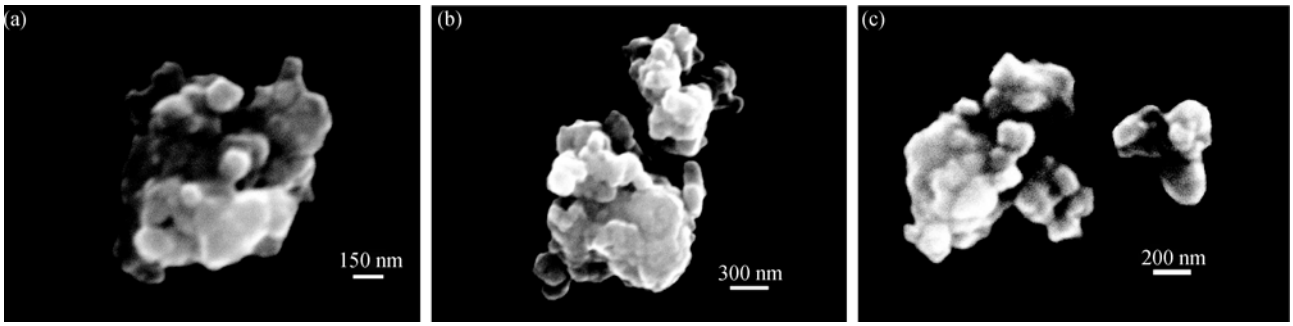

Fig. 5. SEM micrographs of $Ce_{1-x}Zn_xO_{2-x}$ samples obtained at 300°C for 2 h: (a) CeO_2; (b) $Ce_{0.7}Zn_{0.3}O_{1.7}$; (c) $Ce_{0.5}Zn_{0.5}O_{1.5}$.

3.5. Catalytic ability of products

The catalytic ability of ZnO-doped ceria obtained at 300°C for 2 h for air oxidation of castor oil at 125°C is shown in Fig. 6. It can be observed that the catalytic ability of ZnO-doped ceria for air oxidation of castor oil at 125°C was decreased substantially, and increasing the molar ratio of Zn^{2+} to Ce^{4+} can increase the time needed for oxidation of

castor oil. Yabe *et al.* [6] considered that the catalytic activity of ceria must have been related to the oxygen release and absorption equilibrium reaction shown by

$$CeO_2 \rightleftharpoons Ce^{4+}_{1-x}Ce^{3+}_{x}O_{2-x/2}\square_{x/2} + \frac{x}{4}O_2 \quad (1)$$

where □ is the oxygen defect and $0 < x < 1$.

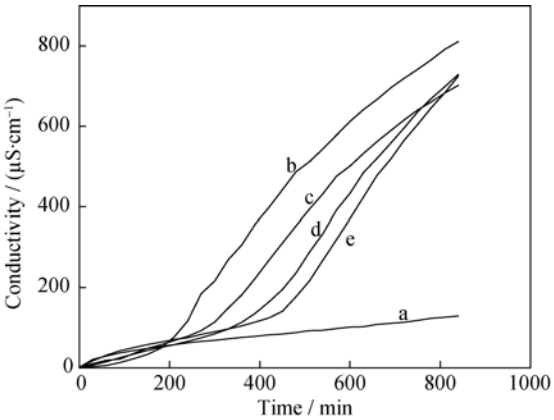

Fig. 6. Evaluation of oxidation catalytic ability at 125°C with the Rancimat systems: (a) blank (without any sample); (b) CeO_2; (c) $Ce_{0.9}Zn_{0.1}O_{1.9}$; (d) $Ce_{0.7}Zn_{0.3}O_{1.7}$; (e) $Ce_{0.5}Zn_{0.5}O_{1.5}$.

By doping an ion with a lower valence and larger ionic size than Ce^{4+}, the fluorite structure of ceria can be stabilized and consequently the oxidation catalytic activity can be reduced. However, Zn^{2+} possesses a smaller ionic size than Ce^{4+}, and the low oxidation catalytic activity of Zn^{2+}-doped CeO_2 is suspected to be mainly due to the formation of the oxygen defect in CeO_2.

4. Conclusions

When $Ce(SO_4)_2{\cdot}4H_2O$, $ZnSO_4{\cdot}7H_2O$, and NH_4HCO_3 were used as starting materials, superfine $Ce_{1-x}Zn_xO_{2-x}$ samples were obtained via a solid-state reaction at room temperature. The ZnO-doped CeO_2 can facilitate formation of crystalline state CeO_2. The results of UV-vis analysis suggest that all ZnO-doped CeO_2 powders still have strong UV absorption ability between 280 and 400 nm. The catalytic ability of ZnO-doped ceria for air oxidation of castor oil at 125°C was decreased substantially. Therefore, the superfine cerium-zinc oxides would have a better future as sunscreen.

Acknowledgements

This work was financially supported by the Natural Scientific Foundation of Guangxi Province (No. 0832111), the Large Apparatus Cooperation Community Net Foundation of Guangxi Province, China (No. 695-2008-108), and the Undergraduate Innovation Foundation of School of Chemistry and Chemical Engineering of Guangxi University.

References

[1] Asano S., Science of sunscreens, *Hyoumenkagaku,* 1994, **15**: 473.

[2] Masaki H., Skin damage induced by solarlight exposure and problems of sunscreen in the 21st century, *Fragrance J.*, 1998, **26**: 65.

[3] Neades R., Cox L., and Pelling J.C., S-phase arrest in mouse keratinocytes exposed to multiple doses of ultraviolet B/A radiation, *Mol. Carcinog.*, 1998, **23**: 159.

[4] He Q., Yin S., and Sato T., Synthesis and photochemical properties of zinc-aluminum layered double hydroxide/organic UV ray absorbing molecule/silica nanocomposites, *J. Phys. Chem. Solids*, 2004, **65**: 395.

[5] Dransfield G.P., Inorganic sunscreens, *Radiat. Prot. Dosim.*, 2000, **91**: 271.

[6] Yabe S. and Sato T., Cerium oxide for sunscreen cosmetics, *J. Solid State Chem.*, 2003, **171**: 7.

[7] El-Toni A.M., Shu Yin S., and Sato T., Synthesis and silica coating of calcia-doped ceria/plate-like titanate ($K_{0.8}Li_{0.27}Ti_{1.73}O_4$) nanocomposite by seeded polymerization technique, *Mater. Chem. Phys.*, 2007, **103**: 345.

[8] Masui T., Hirai H., Imanaka N., and Adachi G., New sunscreen materials based on amorphous cerium and titanium phosphate, *J. Alloys Compd.*, 2006, **408-412**: 1141.

[9] Wu W.W., Fan Y.J., Wu X.H, Liao S., Huang X.F, and Li X.H., Preparation of nano-sized cerium and titanium pyrophosphates via solid-state reaction at room temperature and study on their UV absorbency, *Rare Met.*, 2009, **28**: 33.

[10] Fujishima A. and Honda K., Electrochemical photolysis of water at a semiconductor electrode, *Nature*, 1972, **238**: 37.

[11] Herrmann J.M., Guillard C., and Pichat P., Heterogeneous photocatalysis: an emerging technology for water treatment, *Catal. Today*, 1993, **17**: 7.

[12] Trovarelli A. *Catalysis by Ceria and Related Materials*, Imperial College Press, London, 2002.

[13] Ahmed M.E.T., Shu Y., Shinryo Y., Tsugio S., Coating of calcia-doped ceria with amorphous silica shell by seeded polymerization technique, *Mater. Res. Bull.*, 2005, **40**: 1059.

[14] Li R., Yabe S., Yamashita M., Momose S., Yoshida S., Yin S., and Sato T., UV-shielding properties of zinc oxide-doped ceria fine powders derived via soft solution chemical routes, *Mater. Chem. Phys.*, 2002, **75**: 39.

[15] El-Toni A.M., Yin S., and Sato T., Synthesis and silica coating of calcia-doped ceria/mica nanocomposite by seeded polymerization technique, *Appl. Surf. Sci.*, 2006, **252**: 5063.

[16] Xin X.Q. and Zheng L.M., Solid state reactions of coordination compounds at low heating temperatures, *J. Solid State Chem.*, 1993, **106**: 451.

[17] Yabe S., Yamashita M., Momose S., Tahira K., Yoshida S., Li R., Yin S., and Sato T., Synthesis and UV-shielding properties of metal oxide doped ceria via soft solution chemical processes, *Int. J. Inorg. Mater.*, 2001, **3**: 1003.

[18] Wu W.W. and Jiang Q.Y., Preparation of nano-crystalline zinc carbonate and zinc oxide via solid state reaction at room temperature, *Mater. Lett.*, 2006, **60**: 2791.